

Modeling Galaxy-Galaxy Weak Lensing with SDSS Groups

Ran Li^{1,2*}, H.J. Mo², Zuhui Fan¹, Marcello Cacciato³, Frank C. van den Bosch³, Xiaohu Yang⁴, Surhud More³

¹*Department of Astronomy, Peking University, Beijing 100871, China*

²*Department of Astronomy, University of Massachusetts, Amherst MA 01003, USA*

³*Max-Planck Institute for Astronomy, Königstuhl 17, D-69117 Heidelberg, Germany*

⁴*Shanghai Astronomical Observatory, the Partner Group of MPA, Nandan Road 80, Shanghai 200030, China*

ABSTRACT

We use galaxy groups selected from the Sloan Digital Sky Survey (SDSS) together with mass models for individual groups to study the galaxy-galaxy lensing signals expected from galaxies of different luminosities and morphological types. We compare our model predictions with the observational results obtained from the SDSS by Mandelbaum et al. (2006) for the same samples of galaxies. The observational results are well reproduced in a Λ CDM model based on the WMAP 3-year data, but a Λ CDM model with higher σ_8 , such as the one based on the WMAP 1-year data, significantly over-predicts the galaxy-galaxy lensing signal. We model, separately, the contributions to the galaxy-galaxy lensing signals from different galaxies: central versus satellite, early-type versus late-type, and galaxies in haloes of different masses. We also examine how the predicted galaxy-galaxy lensing signal depends on the shape, density profile, and the location of the central galaxy with respect to its host halo.

Key words: dark matter - large-scale structure of the universe - galaxies: haloes - methods: statistical

1 INTRODUCTION

According to the current paradigm of structure formation, galaxies form and reside inside extended cold dark haloes. While the formation and evolution of dark matter haloes in the cosmic density field is mainly determined by gravitational processes, the formation and evolution of galaxies involves much more complicated, and poorly understood processes, such as radiative cooling, star formation, and all kinds of feedback. One important step in understanding how galaxies form and evolve in the cosmic density field is therefore to understand how the galaxies of different physical properties occupy dark matter haloes of different masses. Theoretically, the connection between galaxies and dark matter haloes can be studied using numerical simulations (e.g., Katz, Weinberg & Hernquist 1996; Pearce et al. 2000; Springel 2005; Springel et al. 2005) or semi-analytical models (e.g. White & Frenk 1991; Kauffmann et al. 1993, 2004; Somerville & Primack 1999; Cole et al. 2000; van den Bosch 2002; Kang et al. 2005; Croton et al. 2006). These approaches try to model the process of galaxy formation from first principles. However, since our understanding of the relevant processes is still poor, the predicted connection between the properties of galaxies and dark matter haloes

needs to be tested against observations. More recently, the halo occupation model has opened another avenue to probe the galaxy-dark matter halo connection (e.g. Jing, Mo & Börner 1998; Peacock & Smith 2000; Berlind & Weinberg 2002; Cooray & Sheth 2002; Scranton 2003; Yang, Mo & van den Bosch 2003; van den Bosch, Yang & Mo 2003; Yan, Madgwick & White 2003; Tinker et al. 2005; Zheng et al. 2005; Cooray 2006; Vale & Ostriker 2006; van den Bosch et al. 2007). This technique uses the observed galaxy luminosity function and clustering properties to constrain the average number of galaxies of given properties that occupy a dark matter halo of given mass. Although the method has the advantage that it can yield much better fits to the data than the semi-analytical models or numerical simulations, one typically needs to assume a somewhat ad-hoc functional form to describe the halo occupation model.

A more direct way of studying the galaxy-halo connection is to use galaxy groups¹, provided that they are defined as sets of galaxies that reside in the same dark matter halo. Recently, Yang et al. (2005; 2007) have developed a halo-based group finder that is optimized for grouping galaxies that reside in the same dark matter halo. Using mock galaxy

¹ In this paper, we refer to a system of galaxies as a group regardless of its richness, including isolated galaxies (i.e., groups with a single member) and rich clusters of galaxies.

* E-mail: ranl@astro.umass.edu

redshift surveys constructed from the conditional luminosity function model (e.g. Yang et al. 2003) and a semi-analytical model (Kang et al. 2005), it is found that this group finder is very successful in associating galaxies with their common dark matter haloes (see Yang et al. 2007; hereafter Y07). The group finder also performs reliably for poor systems, including isolated galaxies in small mass haloes, making it ideally suited for the study of the relationship between galaxies and dark matter haloes over a wide range of halo masses. However, in order to interpret the properties of the galaxy systems in terms of dark matter haloes, one needs to know the halo mass associated with each of the groups. One approach commonly adopted is to use some halo mass indicator (such as the total stellar mass or luminosity contained in member galaxies) to rank the groups. With the assumption that the corresponding halo masses have the same ranking and that the mass function of the haloes associated with groups is the same as that given by a model of structure formation, one can assign a halo mass to each of the observed groups. This approach was adopted by Y07 for the group catalogue used in this paper. There are three potential problems with this approach. First, the approach is model-dependent, in the sense that the assumption of a different model of structure formation will lead to a different halo mass function, and hence assign different masses to the groups. Second, even if the assumed model of structure formation is correct, it is still not guaranteed that the mass assignment based on the ranking of group stellar mass (or luminosity) is valid. Finally, even if all groups are assigned with accurate halo masses, the question how dark matter is distributed within the galaxy groups remains open. Clearly, it is important to have independent mass measurements of the haloes associated with galaxy groups to test the validity of the mass estimates based on the stellar mass (luminosity) ranking.

Gravitational lensing observations, which measure the image distortions of background galaxies caused by the gravitational field of the matter distribution in the foreground, provide a promising tool to probe the dark matter distribution directly. In particular, galaxy-galaxy weak lensing, which focuses on the image distortions around lensing galaxies, can be used to probe the distribution of dark matter around galaxies, hence their dark matter haloes. The galaxy-galaxy lensing signal produced by individual galaxies is usually very weak, and so one has to stack the signal from many lens galaxies to have a statistical measurement. The first attempt to detect such galaxy-galaxy lensing signal was reported by Tyson et al. (1984). More recently, with the advent of wide and deep surveys, galaxy-galaxy lensing can be studied for lens galaxies of different luminosities, stellar masses, colors and morphological types (e.g. Brainerd et al. 1996; Hudson et al. 1998; McKay et al. 2001; Hoekstra et al. 2003; Hoekstra 2004; Sheldon et al. 2004; Mandelbaum et al. 2005, 2006; Sheldon et al. 2007a; Johnston et al. 2007; Sheldon et al. 2007b; Mandelbaum et al. 2008). Given that galaxies reside in dark matter haloes, these results provide important constraints on the mass distribution associated with galaxies in a statistical way.

In this paper, we use the galaxy groups of Y07 selected from the Sloan Digital Sky Survey (SDSS), together with mass models for individual groups, to predict the galaxy-galaxy lensing signal expected from SDSS galaxies. We compare our model predictions with the observational results

obtained by Mandelbaum et al. (2006) for the same galaxies. Our goal is threefold. First, we want to test whether the method of halo-mass assignment to groups adopted by Y07 is reliable. Since the method provides a potentially powerful way to obtain the halo masses associated with the galaxy groups, the test results have general implications for the study of the relationship between galaxies and dark matter haloes. Second, we want to examine in detail the contributions to the galaxy-galaxy lensing signal from different systems, such as central versus satellite galaxies, early-type versus late-type galaxies, and groups of different masses. Such analysis can help us interpreting the observational results. Finally, we would like to study how the predicted galaxy-galaxy lensing signal depends on model assumptions, such as the cosmological model and the density profiles of dark matter haloes. In a companion paper (Cacciato et al. 2008, hereafter C08), we use the relationship between galaxies and dark matter haloes obtained from the conditional luminosity function (CLF) modeling (Yang et al. 2003; van den Bosch et al. 2007) to predict the galaxy-galaxy cross correlation and to calculate the lensing signal, while here we directly use the observed galaxy groups and their galaxy memberships.

This paper is organized as follows. In Section 2 we define the statistical measure that characterizes the galaxy-galaxy lensing effect expected from the mass distribution associated with the galaxy groups. We provide a brief description of the galaxy group catalogue and the models of the mass distribution associated with galaxy groups in Section 3. We present our results in Section 4 and conclude in Section 5. Unless specified otherwise, we adopt a Λ CDM cosmology with parameters given by the WMAP 3-year data (Spergel et al. 2007, hereafter WMAP3 cosmology) in our analysis: $\Omega_m = 0.238$, $\Omega_\Lambda = 0.762$, and $h \equiv H_0/(100 \text{ km s}^{-1} \text{ Mpc}^{-1}) = 0.73$, $\sigma_8 = 0.75$.

2 GALAXY-GALAXY LENSING

Galaxy-galaxy lensing provides a statistical measure of the profile of the tangential shear, $\gamma_t(R)$, averaged over a thin annulus at the projected radius R around the lens galaxies. This quantity is related to the excess surface density (hereafter ESD) around the lens galaxy, $\Delta\Sigma$, as

$$\Delta\Sigma(R) = \gamma_t(R)\Sigma_{\text{crit}} = \bar{\Sigma}(< R) - \Sigma(R), \quad (1)$$

where $\bar{\Sigma}(< R)$ is the average surface mass density within R , and $\Sigma(R)$ is the azimuthally averaged surface density at R . Note that, according to this relation, $\Delta\Sigma(R)$ is independent of a uniform background. In the above equation,

$$\Sigma_{\text{crit}} = \frac{c^2}{4\pi G} \frac{D_s}{D_l D_{ls}(1+z_l)^2} \quad (2)$$

is the critical surface density in comoving coordinates, with D_s and D_l the angular distances of the lens and source, D_{ls} the angular distance between the source and the lens, and z_l the redshift of the lens.

By definition, the surface density, $\Sigma(R)$, is related to the projection of the galaxy-matter cross-correlation function, $\xi_{g,m}(r)$, along the line-of-sight. In the distant observer approximation

$$\Sigma(R) = \bar{\rho} \int_{-\infty}^{\infty} \left[1 + \xi_{g,m}(\sqrt{R^2 + \chi^2}) \right] d\chi, \quad (3)$$

where $\bar{\rho}$ is the mean density of the universe and χ is the line-of-sight distance from the lens.

The cross-correlation between galaxies and dark matter can, in general, be divided into a 1-halo term and a 2-halo term. The 1-halo term measures the cross-correlation between galaxies and dark matter particles in their own host haloes, while the 2-halo term measures the cross-correlation between galaxies and dark matter particles in other haloes. In the present work, we are interested in the lensing signals on scales $R \leq 2h^{-1}\text{Mpc}$ where the observational measurements are the most accurate. As we will show in § 4, on such scales the signal is mainly dominated by the 1-halo term. Nevertheless, our model also takes the contribution of the 2-halo term into account. More importantly, since central galaxies (those residing at the center of a dark matter halo) and satellite galaxies (those orbiting around a central galaxy) contribute very different lensing signals (e.g. Natarajan, Kneib & Smail 2002; Yang et al. 2006; Limousin et al. 2007), it is important to model the contributions from central and satellite galaxies separately.

As an illustration, in Fig. 1 we show the ESDs expected from a single galaxy in a host halo of mass $10^{14}h^{-1}M_{\odot}$. The solid line represents the lensing signal expected for the central galaxy of the halo. While the dotted and dashed lines show the lensing signal of a satellite galaxy residing in a sub-halo of $10^{11}h^{-1}M_{\odot}$ with a projected halo-centric distance $r_p = 0.2h^{-1}\text{Mpc}$ and $r_p = 0.4h^{-1}\text{Mpc}$ from the center of the host halo, respectively. In the calculation, the dark matter mass distribution in the host halo is assumed to follow the Navarro, Frank & White (1997) profile and that in the sub-haloes is assumed to follow the Hayashi et al. (2003) model. These models are described in detail in § 3.3. In order to estimate the ESD, we sample these profiles with mass particles and project the positions of all particles to a plane perpendicular to the line of sight. The $\Sigma(R)$ is then estimated by counting the number of dark matter particles in an annulus with radius R centred on the selected galaxies. Fig. 1 shows clearly that the lensing signals of the central and the satellite are quite different. The ESD of the central galaxy follows the mass distribution of the host halo, decreasing monotonically with R . The ESD of a satellite, on the other hand, consists of two parts: one from the sub-halo associated the satellite, which contributes to the inner part, and the other from the host halo, which dominates at larger R . This simple model demonstrates clearly that, in order to model the galaxy-galaxy lensing signal produced by a population of lens galaxies, one needs to model carefully the distribution of matter around both host haloes and sub-haloes. To do this, we need not only to identify the haloes in which each lens galaxy resides, but also to model the mass and density profile of each host halo and subhalo. In addition we also need to model the distribution of dark matter relative to galaxies. In the following section, we describe our modeling with the use of observed galaxy groups.

3 MODELING THE MASS DISTRIBUTION ASSOCIATED WITH THE SDSS GROUPS

3.1 The SDSS Group Catalogue

Our analysis is based on the SDSS galaxy group catalogue constructed by Y07. The groups are selected with the adap-

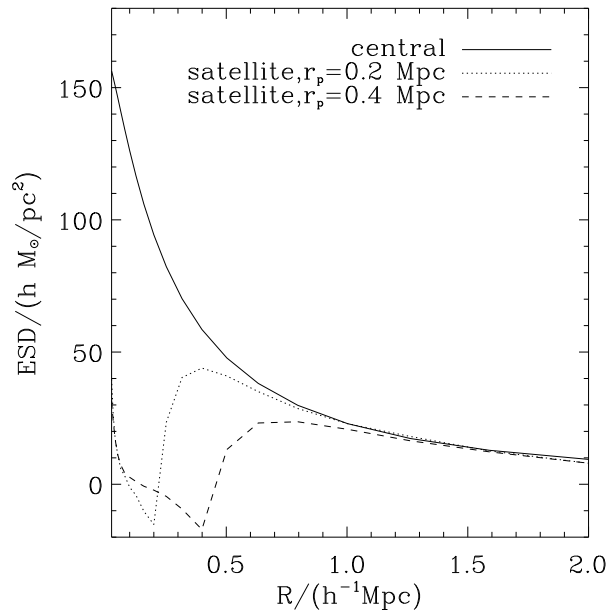


Figure 1. The ESD expected for a single galaxy. Here the host halo mass is assumed to be $10^{14}h^{-1}M_{\odot}$. The solid line represents the lensing signal for the central galaxy in such a halo. The dotted line represents the lensing signal of a satellite galaxy residing in a sub-halo of mass $10^{11}h^{-1}M_{\odot}$ which has a projected distance $r_p = 0.2h^{-1}\text{Mpc}$ from the center of the host halo. The dashed line is the same as the dotted line, except that the subhalo's projected distance is $0.4h^{-1}\text{Mpc}$ from the center of the host halo.

tive halo-based group finder developed by Yang et al. (2005), from the New York University Value Added Galaxy Catalog (NYU-VAGC; Blanton et al. 2005) which is based on the SDSS Data Release 4 (Adelman-McCarthy et al. 2006). Only galaxies with redshifts in the range $0.01 \leq z \leq 0.2$, and with redshift completeness $\mathcal{C} > 0.7$, are used in the group identification. The magnitudes and colors of all galaxies are based on the standard SDSS Petrosian technique (Petrosian 1976; Strauss et al. 2002), and have been corrected for galactic extinction (Schlegel, Finkbeiner & Davis 1998). All magnitudes have been K-corrected and evolution-corrected to $z = 0.1$ following the method described in Blanton et al. (2003). In Y07, three group samples were constructed using galaxy samples of different sources of galaxy redshifts. Our analysis is based on Sample II, which includes 362,356 galaxies with redshifts from the SDSS and 7091 galaxies with redshifts taken from alternative surveys: 2dFGRS (Colless et al. 2001), PS0z (Saunders et al. 2000) or from the RC3 (de Vaucouleurs et al. 1991). There are in total 301,237 groups, including those with only one member galaxy. The group finder has been applied to mock catalogue to test the completeness and purity of the groups in Y07. About 90% of the groups have a completeness $f_c > 0.6$ and 80% groups with $f_c > 0.8$, where f_c is defined as the ratio between the number of true members that are selected as the members of the group and the number of the total true members of the group.

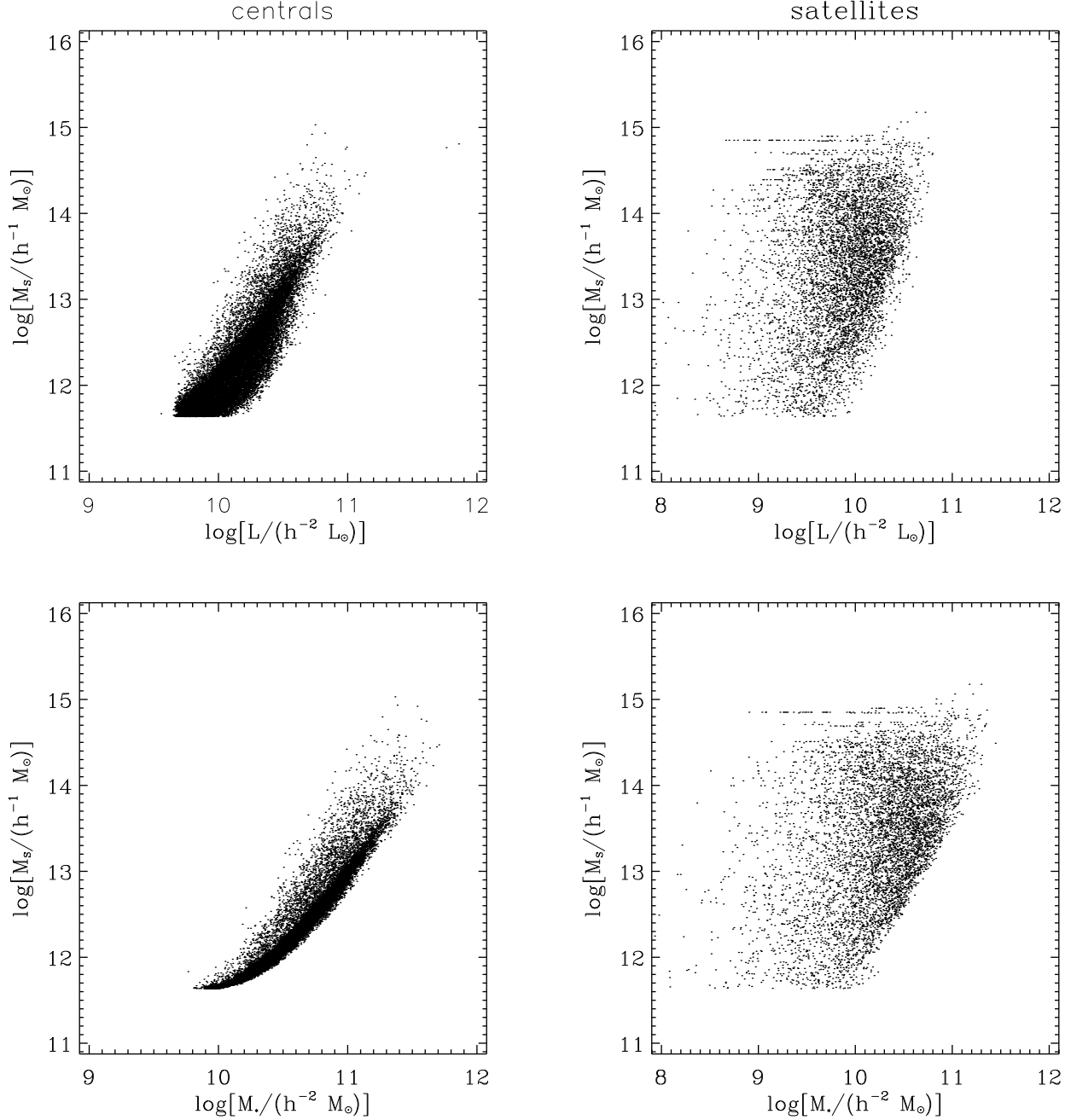


Figure 2. The halo mass M_S (estimated using stellar mass), versus M_* (lower panels) and L (upper panels) of the galaxies in the haloes. The left panels are for central galaxies and the right panels are for satellite galaxies.

3.2 Halo Mass Assignment

An important aspect of the group catalog construction is the determination of the halo mass, M_{vir} , of each group. In Y07, two estimators are adopted. The first, M_L , is estimated using the ranking of the characteristic luminosity of a group, which is the total luminosity of all member galaxies in the group with $M_r - 5 \log h \leq -19.5$ (hereafter referred to as $L_{19.5}$). The second, M_S , is estimated using the ranking of the characteristic stellar mass, M_{stellar} which is defined to be the total stellar mass of group members with $M_r - 5 \log h \leq -19.5$. For each galaxy the stellar mass is estimated from

its absolute magnitude and color using the fitting formula given by Bell et al. (2003).

The basic assumption of the ranking method is that there is a one-to-one relation between M_{stellar} (or $L_{19.5}$) and the group mass. Using the dark matter halo mass function predicted by a model of structure formation, one can assign a halo mass to each group according to its M_{stellar} - ranking (or $L_{19.5}$ - ranking). In this paper, we use the mass function obtained by Warren et al. (2006). Note that this one-to-one mapping is applicable only when the group sample is complete. In Y07, three complete samples are constructed in

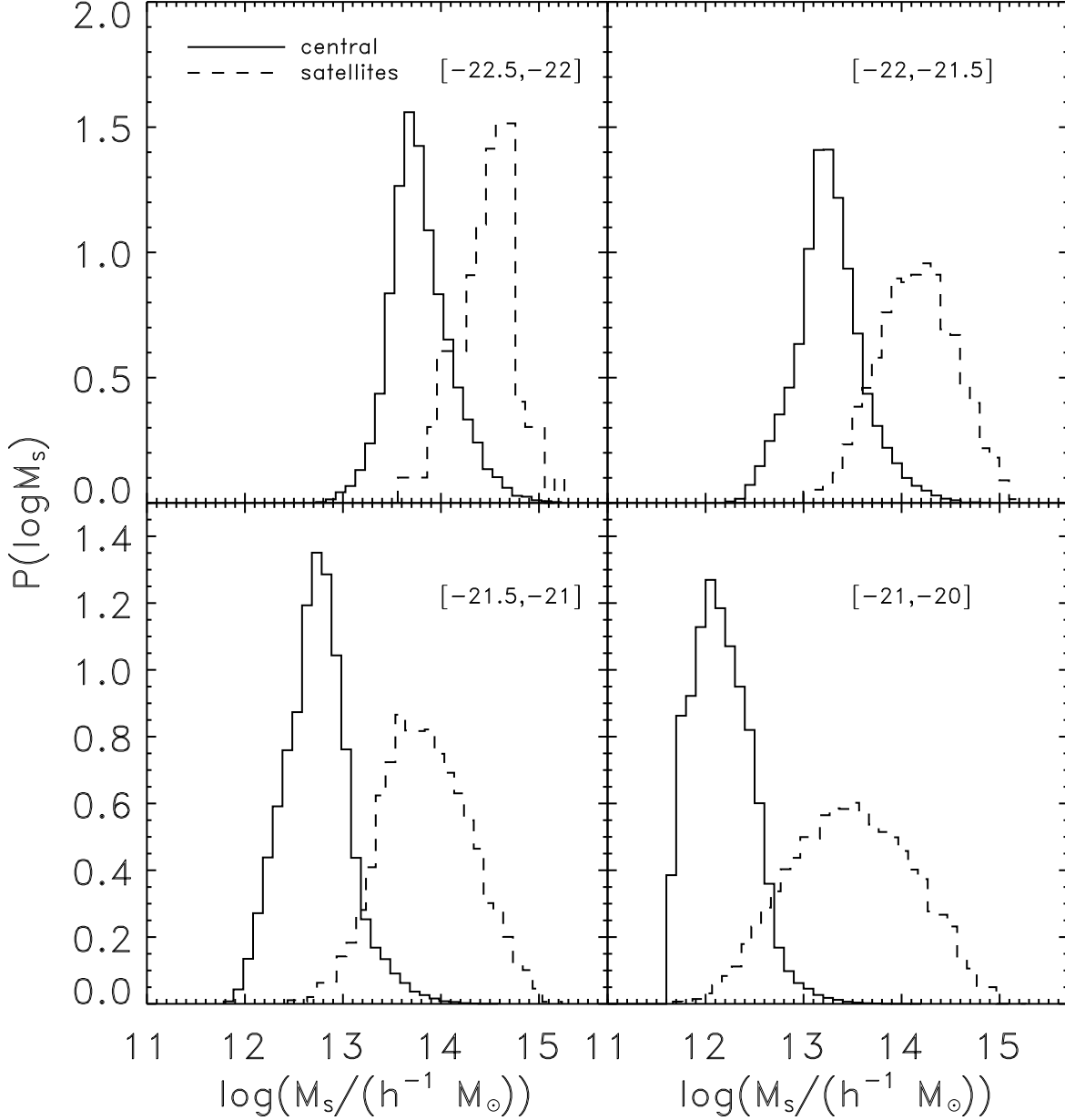


Figure 3. The distribution of the host halo masses for the central and satellite galaxies in different luminosity bins, as indicated by the r -band absolute-magnitude range in each panel.

three redshift ranges. Only groups in the complete samples are used in the ranking. The mass of other groups are estimated by a linear interpolation based on the $M_{\text{stellar}}-M_{\text{vir}}$ relation (or the $L_{19.5} - M_{\text{vir}}$) obtained from the complete sample. Detailed tests using mock galaxy redshift samples have shown that the $1-\sigma$ error of the estimated halo mass is ~ 0.3 dex (Y07). In addition, the two mass estimators, M_L and M_S , agree remarkably well with each other, with a scatter that decreases from about 0.1 dex at the low-mass end to about 0.05 dex at the high-mass end. Since the correlation between M_{stellar} and halo mass is somewhat tighter

than that between $L_{19.5}$ and halo mass, we adopt M_S as our fiducial halo mass throughout. As we demonstrate in § 4.3, using M_L instead yields results that are fairly similar.

Fig. 2 shows the relation between the host halo mass, M_S , and the galaxy stellar mass M_* (the lower two panels) or the galaxy luminosity L (the upper two panels). Results are shown separately for central galaxies (left panels) and satellite galaxies (right panels). As one can see, the stellar mass (luminosity) of central galaxies is quite tightly correlated with their host halo masses. However, for satellite galaxies of a given stellar mass (or luminosity), their host

halo mass covers a very large range, reflecting the fact that many low-mass galaxies are satellites in massive haloes. The distributions of host halo masses, M_S , for central or satellite galaxies in different luminosity bins are shown in Fig. 3. On average, brighter central galaxies reside in more massive haloes. For faint galaxies, the halo-mass distribution is broader, again because many faint galaxies are satellites in massive systems.

In the group catalogue, the mass assignment described above is used only for groups where the brightest galaxy is brighter than $M_r - 5 \log h = -19.5$. This is because the mass ranking used in the group catalog is based on the total stellar mass (or total luminosity) of the member galaxies that are brighter than $M_r - 5 \log h = -19.5$. The groups with no galaxies brighter than this magnitude thus have no assigned rank. As described in Y07, the reason for choosing this magnitude is a compromise between having a complete sample in a relatively large volume and having more groups that are represented by a number of member galaxies. For groups in which all member galaxies have $M_r - 5 \log h > -19.5$, a different method has to be adopted. In modeling the luminosity function and stellar mass function of the central galaxies based on the same SDSS group catalogue as used here, Yang et al. (2008) obtain an average relation between the luminosity (or stellar mass) of the central galaxy and the halo mass down to $M_r - 5 \log h \sim -17$. We adopt this relation to assign halo masses to all groups (including those containing only one isolated galaxy) represented by centrals with $M_r - 5 \log h > -19.5$. For convenience, the halo masses obtained in this way are also referred to as M_S (based on the stellar mass of central galaxies) and M_L (based on the r -band luminosity of the central galaxies), respectively.

3.3 Mass Distribution in Haloes and Subhaloes

With the group catalogue described above, we can model the dark matter distribution by convolving the halo distribution with the density profiles of individual haloes. In our modeling of the density profiles, the host halo of a group is assumed to be centered on the central galaxy. There are two ways to define a central galaxy: one is to define the central in a group to be the galaxy with the highest stellar mass, and the other is to define the central to be the brightest member. For most groups these two definitions give the same results, but there are very few cases (less than $\sim 2\%$) where different central galaxies are defined. In our fiducial model, we define the most massive galaxies (in term of stellar mass) to be the central galaxies.

In a hierarchical model, a dark matter halo forms through a series of merger events. During the assembly of a halo, most of the mass in the merging progenitors is expected to be stripped. However, some of them may survive as subhaloes, although the total mass contained in subhaloes is small, typically $\sim 10\%$ (van den Bosch, Tormen & Giocoli 2005). Some of the subhaloes are associated with ‘satellite galaxies’ in a halo. In our modeling of the galaxy-galaxy weak lensing, we only take into account subhaloes associated with satellite galaxies, treating other subhaloes as part of the host halo. Giocoli, Tormen & van den Bosch (2008) provide a fitting function of the average mass function for subhaloes at the time of their accretion into the parent halo of a given mass. Using this mass function, we first sample

a set of masses for each group mass. We then set the mass originally associated with a satellite galaxy according to the stellar mass ranking of the satellites in the group. Here we implicitly assume that the initial subhalo mass function is the same as the mass function of the subhaloes that host satellites. This assumption is not proved by any observations, and we have to live with it since a more realistic model is not currently available. Fortunately, subhaloes only contribute a small fraction to the total lensing signal on small scales. The uncertainty here will not have a significant impact on any of our conclusions. To obtain the final mass in the subhalo at the present time, the evolution of the subhaloes needs to be taken into account. In other words, we need to know the fraction of the mass that is stripped and how the structure of a subhalo changes after the stripping. Here it is convenient to introduce a parameter f_m which is the retained mass fraction of the subhalo. Gao et al. (2004) studied the radial dependence of the retained mass fraction f_m from a large sample of subhaloes in a large cosmological simulation. In their work, f_m is considered as a function of $r_s/r_{\text{vir,h}}$, where r_s is the distance of the subhalo from the center of the host halo and $r_{\text{vir,h}}$ is the virial radius of the host halo. The simulation of Gao et al. gives

$$f_m = 0.65(r_s/r_{\text{vir,h}})^{2/3}. \quad (4)$$

We will adopt this in our modeling of the masses associated with subhaloes. However, in the group catalogue, only the projected distance, r_p , from the group center is available. The 3D-distance, r_s , is obtained by randomly sampling the NFW profile of the host halo with the given projected radius r_p .

Thus, the mass assigned to a subhalo is determined by the following three factors: (1) the stellar mass of the satellite galaxy; (2) the host halo mass; (3) the distance between the satellite and the center of the host. Here the host halo mass comes into our calculation in two ways. It not only determines the subhalo mass function, but also affects the parameter f_m in Eqs.4. Note that the accretion history of the host halo may also affect the value of f_m . We have to neglect such effect because it is unclear how to model the accretion histories for individual groups.

For host haloes, we use the following NFW profile (Navarro, Frank & White 1997) to model the mass distribution:

$$\rho(r) = \frac{\delta_0 \bar{\rho}}{(r/r_c)(1 + r/r_c)^2}. \quad (5)$$

where $\bar{\rho}$ is the mean density of the universe, r_c is a scale radius, related to virial radius r_{vir} by the concentration, $c = r_{\text{vir}}/r_c$, and δ_0 is a characteristic over-density related to the average over-density of a virialized halo, Δ_{vir} , by

$$\delta_0 = \frac{\Delta_{\text{vir}}}{3} \frac{c^3}{\ln(1+c) - c/(1+c)}. \quad (6)$$

We adopt the value of Δ_{vir} given by the spherical collapse model (see Nakamura & Suto 1997; Henry 2000). Numerical simulations show that halo concentrations are correlated with halo mass, and we use the relations given by Macciò et al. (2007), converted to our definition of halo mass. Note that here we use r_c , instead of the conventional notation r_s , to denote the scale radius of the NFW profile, as r_s has been used to denote the distance of a subhalo from the center of its host.

For sub-haloes, we model their density profiles using the results obtained by Hayashi et al. (2003), who found that the density profiles of stripped sub-haloes can be approximated as

$$\rho_s(r) = \frac{f_t}{1 + (r/r_{t,\text{eff}})^3} \rho(r), \quad (7)$$

where f_t is a dimensionless factor describing the reduction in the central density, and $r_{t,\text{eff}}$ is a cut-off radius imposed by the tidal force of the host halo. For $f_t = 1$ and $r_{t,\text{eff}} \gg r_c$, $\rho_s(r)$ reduces to the standard NFW profile $\rho(r)$. Here $\rho(r)$ is calculated using the mass of the subhalo at the time of its accretion into the host halo. Both f_t and $r_{t,\text{eff}}$ depend on the mass fraction of the sub-halo that remains bound, f_m . Based on N -body simulations, Hayashi et al. obtained the following fitting formulae relating f_t and $r_{t,\text{eff}}$ to f_m :

$$\log(r_{t,\text{eff}}/r_c) = 1.02 + 1.38 \log f_m + 0.37(\log f_m)^2; \quad (8)$$

$$\log(f_t) = -0.007 + 0.35 \log f_m + 0.39(\log f_m)^2 + 0.23(\log f_m)^3. \quad (9)$$

It should be pointed out, though, that there are substantial uncertainties in modeling the mass distribution around individual satellite galaxies. In particular, many of the results about subhaloes are obtained from N -body simulations, and it is unclear how significant the effect of including baryonic matter is. Fortunately, the total mass associated with satellite galaxies is small (see e.g. Weinberg et al. 2008). Furthermore, the contribution of the subhaloes associated with the satellite galaxies to the galaxy-galaxy lensing signal is confined to small scales. We therefore expect that these uncertainties will not change our results significantly.

With the mass distributions described above, we use a Monte-Carlo method to sample each of the profiles with a random set of mass particles. Note that the halo mass assigned to a group in the SDSS Group Catalog is M_{180} , which is the mass enclosed in the radius, r_{180} , defined such that $M_{180} = 4\pi r_{180}^3(180\bar{\rho})/3$. We therefore sample the particle distribution within r_{180} . After all the particles in each halo are sampled, we project the positions of all the particles to a plane and calculate $\Delta\Sigma(R)$ by stacking galaxies in each of the luminosity bin. Since the mass distribution is isotropic, an arbitrary direction can be chosen for the stacking. Thus, the projection effect is naturally included in our calculation. Each of the particles has a mass of $10^{10} h^{-1} M_\odot$. Our test using particles of lower masses shows that the mass resolution adopted here is sufficient for our purpose. Using 2 times more particles leads to a difference of about 5% at $R \sim 0.02 h^{-1} \text{Mpc}$, and almost no difference at $R \geq 0.1 h^{-1} \text{Mpc}$.

4 RESULTS

4.1 SDSS Lensing Data

Before presenting our model predictions, we first describe the observational results that we will use for comparison. The observational results to be used were obtained by Mandelbaum et al. (2006), who analyzed the galaxy-galaxy lensing effects using galaxies in a sample constructed from the SDSS DR4 spectroscopic sample. Their sample of lensing

Table 1. The properties of galaxy samples. In each case, the absolute-magnitude range, the mean redshift, the mean luminosity, and the fraction of late-types are listed. Note that $L_* = 1.2 \times 10^{10} h^{-2} L_\odot$

Sample	M_r	$\langle z \rangle$	$\langle L/L_* \rangle$	f_{late}
L1	$-18 < M_r < -17$	0.031	0.075	0.81
L2	$-19 < M_r < -18$	0.048	0.191	0.70
L3	$-20 < M_r < -19$	0.074	0.465	0.54
L4	$-21 < M_r < -20$	0.111	1.13	0.35
L5f	$-21.5 < M_r < -21$	0.145	2.09	0.22
L5b	$-21.5 < M_r < -22$	0.150	3.22	0.12
L6f	$-22 < M_r < -22.5$	0.152	5.01	0.04

galaxies is similar to the galaxy sample used in Y07 to construct the group catalogue used here. The only difference is that Mandelbaum et al.'s sample includes all galaxies with redshifts in the range $0.02 < z < 0.35$, while the galaxies in Y07's group catalogue are in $0.01 \leq z \leq 0.2$. Since, as to be described below, we are interested in the lensing signals around galaxies of given luminosity and morphological type, this difference in redshift range is not expected to have a significant impact on our results. For the faint luminosity bins, our galaxy samples should be almost identical to that of Mandelbaum et al. (2006), because all faint galaxies are at $z \leq 0.2$ in the SDSS catalog. For bright galaxies we also expect the statistic properties of the two samples to be similar. Both Mandelbaum et al. (2006) and Y07 applied similar evolution correction and K correction, so that the evolution in the galaxy population has been taken into account, albeit in a simple way. As we will see, even for the two brightest bins, the lensing signal is dominated by halos with masses $\sim 10^{14} h^{-1} M_\odot$, and the change in the halo mass function around this mass is small between $z = 0.2$ and 0.35 . Following Mandelbaum et al. (2006), we split the galaxy sample into 7 subsamples according to galaxy luminosity. Table 1 shows the properties of these subsamples: the luminosity range covered by each subsample, the mean redshift, the mean luminosity, and the fraction of late-type galaxies. As expected the mean redshifts of brightest bins are different from the corresponding redshifts in Mandelbaum et al.

Also following Mandelbaum et al. (2006), we split each galaxy subsample into two according to galaxy morphology. The separation is made according to the parameter $frac_{\text{dev}}$ generated by the PHOTO pipeline. The value of $frac_{\text{dev}}$ is obtained by fitting the galaxy profile, in a given band, to a model profile given by $frac_{\text{dev}} \times F_{\text{dev}} + (1 - frac_{\text{dev}}) \times F_{\text{exp}}$, where F_{dev} and F_{exp} are the de Vaucouleurs and exponential profiles, respectively. As in Mandelbaum et al., we use the average of $frac_{\text{dev}}$ in the g , r and i bands. Galaxies with $frac_{\text{dev}} \geq 0.5$ are classified as early-type, while those with $frac_{\text{dev}} < 0.5$ as late-type.

It should be pointed out that we did not carry a ray-tracing simulation to predict the galaxy-galaxy lensing results. Instead, we directly calculate the excess surface density around SDSS galaxies. Thus, our calculation doesn't deal with source galaxies. On the other side, in Mandelbaum et al. (2006) the source galaxies are carefully weighted, and lensing signals are calibrated, to reduce any bias in the observational measurements (see Mandelbaum et al. 2005 for

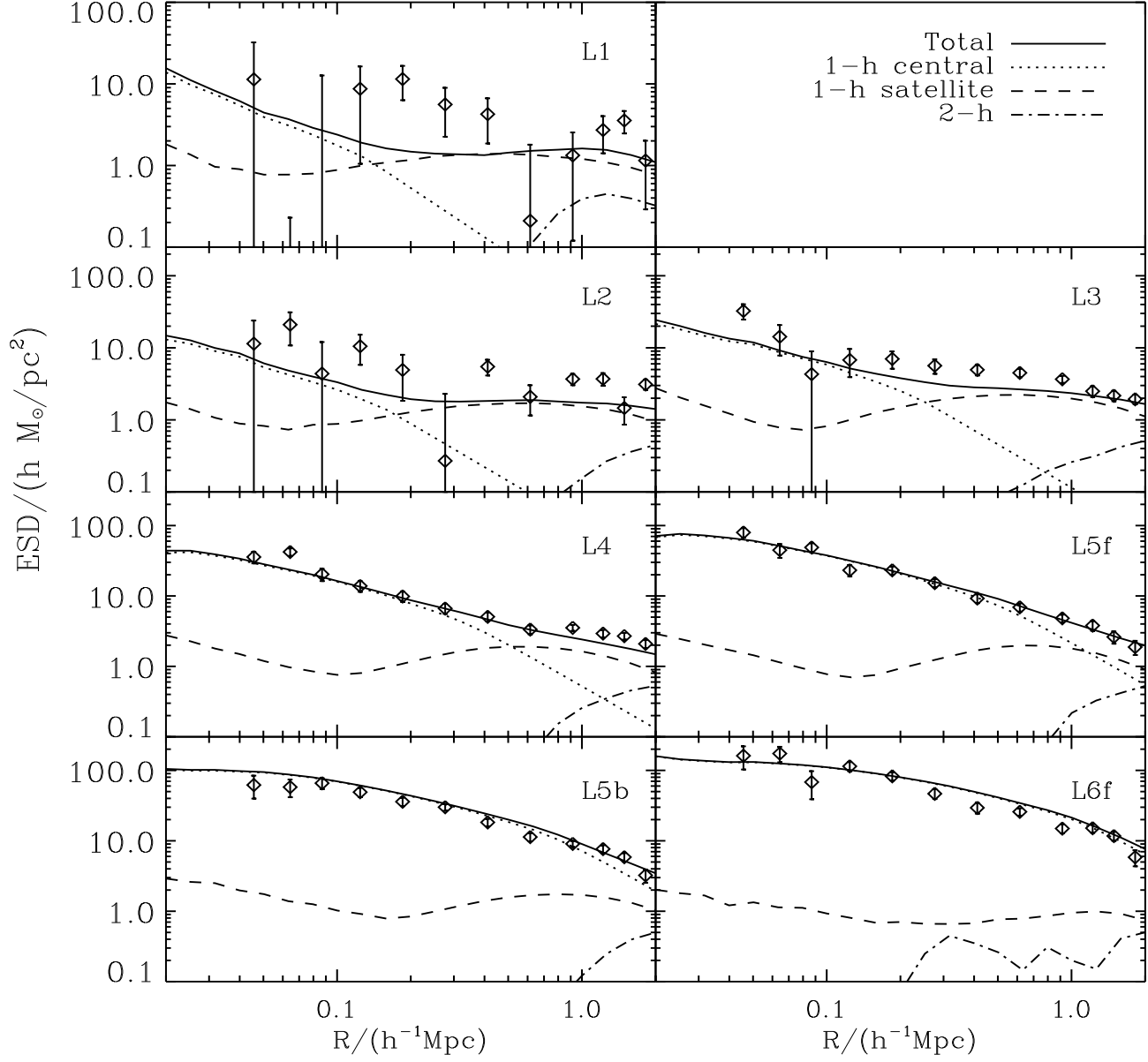


Figure 4. Comparison of the lensing signal predicted by the fiducial model with the observational results. Here the ESD is plotted as the function of the transverse distance R for lensing galaxies in different luminosity bins. Data points with error bars are the observational results of Mandelbaum et al. , while the lines are the model predictions. The dotted, dashed and dot-dashed lines represent the contributions of the ‘1-halo term’ of central galaxies, the ‘1-halo term’ of satellite galaxies, and the ‘2-halo term’ (of both centrals and satellites), respectively. The solid lines show the predicted total ESD. The r -band magnitude range for each case can be found in Table 1.

details). Thus, we assume the observational results are unbiased, and compare them directly with our model predictions.

The observation data used here was kindly provided by R. Mandelbaum. The data used in Fig. 6 has been published in Mandelbaum et al. (2006) where lensing signal is calculated for early and late type galaxies separately. R. Mandelbaum also provided the lensing data combining early and late type galaxies for us to make the comparisons presented in all other figures. Note that here we only show the com-

parison of the lensing signal for galaxies divided according to luminosity.

The errorbars on the observational points are 1σ statistical error. The systematic error of the galaxy-galaxy lensing has been discussed in detail in Mandelbaum et al. (2005). The test has been carried out for three source samples: $r < 21$, $r > 21$, and high redshift LRGs. The overall systematic error is found to be comparable to or slightly larger than the statistical error shown here.

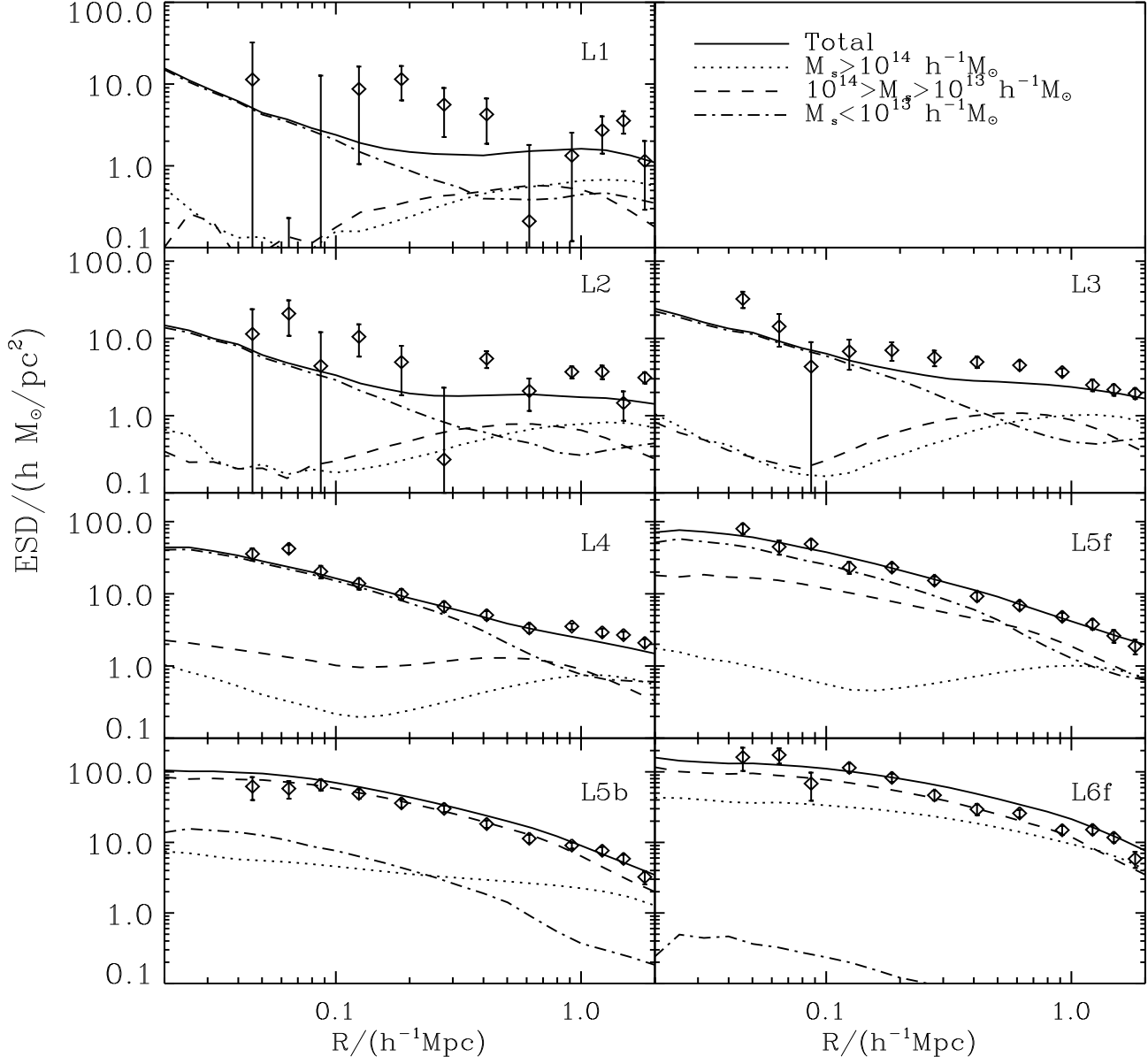


Figure 5. The contribution to the ESD plotted separately for dark matter haloes of different masses. In each panel, the dotted line shows the contribution from haloes with $M_S \geq 10^{14} h^{-1} M_\odot$. The dashed line shows the contribution from haloes with $10^{13} h^{-1} M_\odot \leq M_S < 10^{14} h^{-1} M_\odot$, and the dot-dashed line shows the contribution from haloes with $M_S < 10^{13} h^{-1} M_\odot$. The solid line shows the total lensing signal predicted by the fiducial model. For comparison, the observational data are included as data points with error-bars.

4.2 The Fiducial Model

In Fig. 4 we show the lensing signal around galaxies in different luminosity bins obtained from our fiducial model, which has model parameters as described in the last section and assumes the WMAP3 cosmology. Here the ESD is plotted as a function of the projected distance R from galaxies. The solid line shows the averaged ESD of all galaxies in the corresponding luminosity bin. The amplitude of the predicted ESD increases with galaxy luminosity, reflecting the fact that brighter galaxies on average reside in more massive haloes, as shown in Figs. 2 and 3. These results are to be compared with the data points which show the obser-

vational results obtained by Mandelbaum et al. (2006) for the same luminosity bins. Overall, our fiducial model reproduces the observational data reasonably well, especially for bright galaxy bins where the observational results are the most reliable. The reduced χ^2 is 3.2 combining all the luminosity bins. The best match is for L5f, with a reduced χ^2 of 0.9. Given that we do not adjust any model parameters, the χ^2 indicates a good agreement. For the three low-luminosity bins, the predicted ESD is lower than the corresponding observational result. For L1 and L2, the observational data are very uncertain. For L3, if we take the observational data points at face-value, the discrepancy with

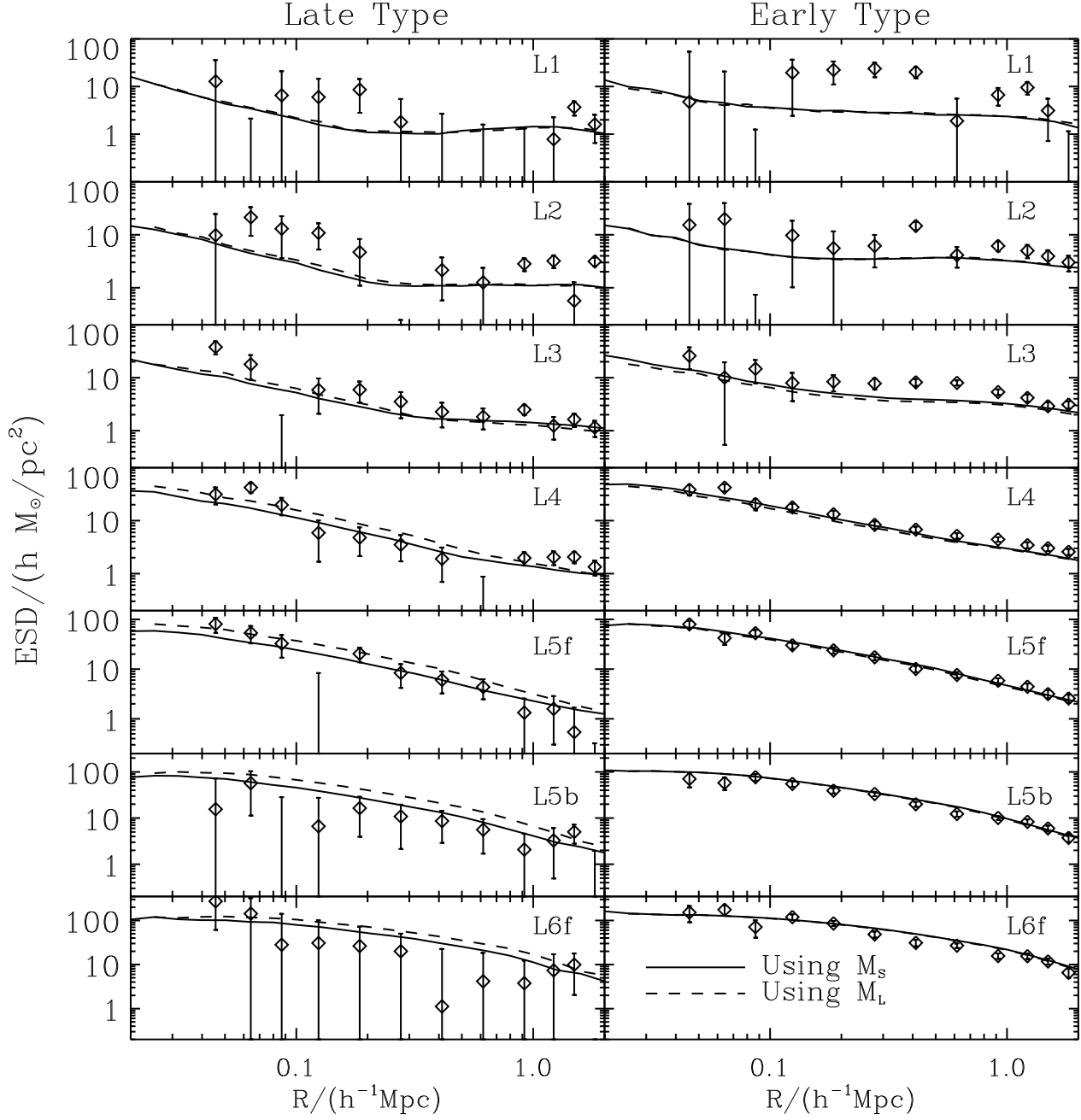


Figure 6. The right panels show the ESD of early galaxies in different luminosity bins, while the left panels show the results for late galaxies. The data points with error-bars show the observational results. The model predictions of the ESD using stellar mass as halo mass indicator are shown as the solid lines. For comparison, the dashed lines show the corresponding model predictions using M_L as the halo masses.

the model prediction is significant. As described in § 3.2, for groups which do not contain any member galaxies with $M_r - 5 \log h < -19.5$, their halo masses are *not* obtained from the ranking of M_{stellar} , but from the average stellar mass-halo mass relation of central galaxies that is required to match the observed stellar mass function of central galaxies. While all the galaxies in the bright luminosity bins have their host halo mass assigned by ranking method, the fraction of the galaxies in halos that have masses assigned according to the mass-halo mass relation is about 30% in L3

and about 70% in L2 and L1. It is possible that this relation underestimates the halo mass. In order to see the effect caused by such uncertainties, we have used a set of parameters from Yang et al. (2008) that are still allowed by the observed stellar mass function but give larger halo masses to the hosts of faint central galaxies. This increases the predicted ESD for L3 by $\sim 20\%$, not sufficient to explain the discrepancy. Indeed, this discrepancy is not easy to fix. In the observational data, the amplitudes of the ESD for L3 at $R \sim 0.3 - 0.9 h^{-1} \text{Mpc}$ are actually slightly higher than

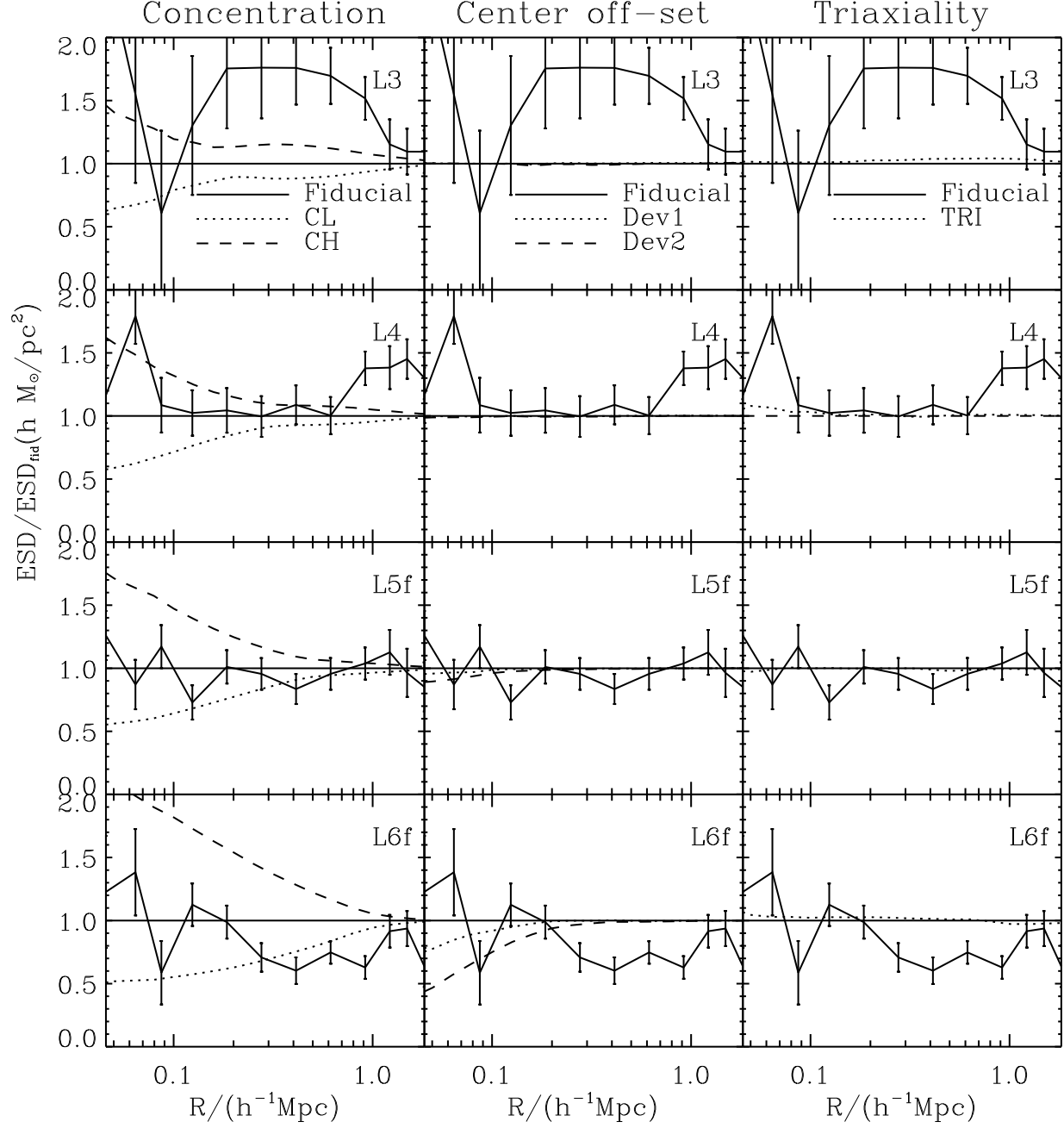


Figure 7. The dependence of the predicted $\Delta\Sigma(R)$ on various model parameters. For comparison, the observational data are included as data points with error-bars. The left column shows the dependence on halo concentration: the halo concentrations in CL (dotted line) and CH (dashed line) are assumed to be 1/2 and 2 times those in the fiducial model (solid line), respectively. The middle column of shows the effects of halo center offset. The dotted line and the dashed line show the results of models Dev1 and Dev2 model, respectively, while the solid line is the fiducial model. The right column shows the effect of assuming triaxial halo density profile. The dotted line shows the result of model TRI, while the solid line again shows the fiducial model. Both the observation and model predicted $\Delta\Sigma(R)$ are normalized by the fiducial prediction.

for the brighter sample L4, while in our model the ESD for L3 is always lower than that for L4. There is an effect that may help to reduce the discrepancy between our model prediction and the observational results for low-mass galaxies. Since the group catalogue is only complete down to certain halo mass limit at different redshift (see Y07), additional assumptions have to be made in order to model the dis-

tribution of the haloes below the mass limit. In the model described above, we have assumed that the haloes below the mass limit have a random distribution, so that they do not contribute to the ESD. However, in reality these low-mass haloes are correlated with the more massive ones. As a result, our assumption will underestimate the 2-halo term of the ESD.

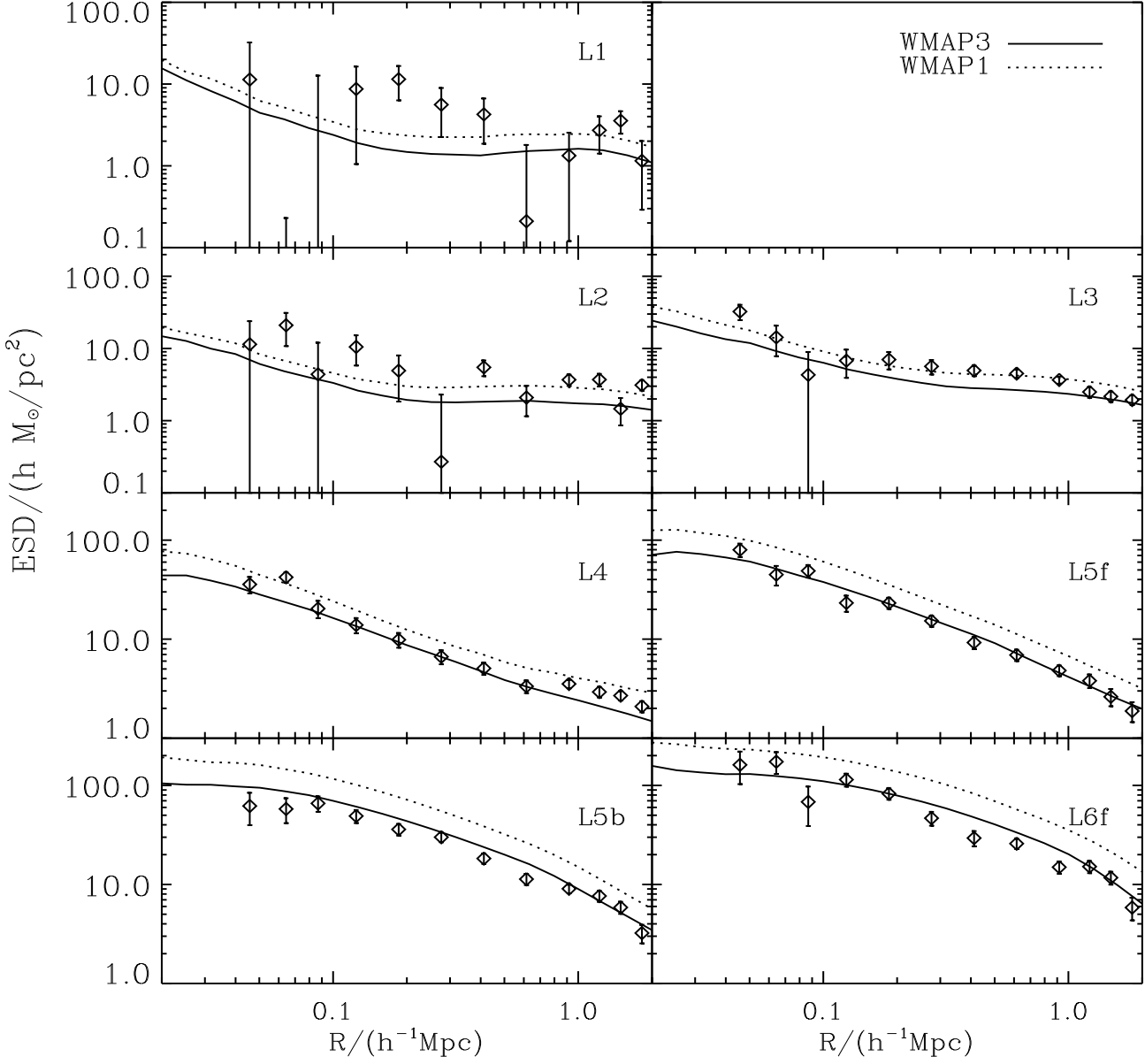


Figure 8. The model prediction of ESD assuming different cosmological models. The solid and dotted lines show the fiducial model and model using WMAP1 parameters, respectively. The observational data are plotted as data points with error-bars.

In order to understand how the predicted ESD is produced, we also show separately the contributions from different sources. The dotted lines show the ESD contributed by the 1-halo term of central galaxies. For all the luminosity bins, this term dominates the ESD at small R . For the brightest two bins, this term dominates the ESD over the entire range of R studied. This reflects the fact that almost all the galaxies in these two bins are central galaxies and the haloes in which they reside are more extended. The dashed lines show the ESD contributed by the 1-halo term of satellite galaxies. This term first decreases with R and then increases to a peak value before declining at large R . This owes to the fact that, in the inner part, the lensing signal produced by satellite galaxies is dominated by the subhaloes

associated with them, while at larger R the lensing signal produced by satellite galaxies is dominated by their host haloes. The value of R at which the ESD reaches the minimum corresponds roughly to the average halo-centric distance of the subhaloes in the luminosity bin. Note that the contribution of satellites to the total ESD is only important at large R in the low-luminosity bins. This reflects the fact that a significant fraction of the low-luminosity satellites reside in massive haloes. Note that although the 1-halo satellite term dominates the lensing signal at $R \geq 0.3 h^{-1} \text{Mpc}$ for faint luminosity bins, the discrepancy between the observation and our prediction cannot be simply solved by boosting up the satellite contribution. The reason is that the increase of the 1-halo satellite term requires the increase of the host halo

mass of the satellites, which will make the 1-halo central term of the bright bins increase as well, causing significant discrepancy for the bright bins. Finally, the dash-dotted lines represent the contribution of the 2-halo term. As expected, this term is relevant only on relatively large scales. In our model this term never dominates at $R \leq 2h^{-1}\text{Mpc}$. However, as discussed before this term may be underestimated here. In C08, the 2-halo term is found to be comparable to the 1-halo satellite term even at $R \sim 0.3h^{-1}\text{Mpc}$. Unfortunately the 2-halo term in C08 may be overestimated because halo-exclusion effect is not properly included.

The large fluctuations seen in L6f are due to the small number of galaxies in this luminosity bin.

Since the halo mass of each lensing galaxy is known in our model, we can also examine the contributions to the total ESD in terms of the halo mass. Fig. 5 shows the results where the host haloes are split into three bins of M_S : $M_S \geq 10^{14}h^{-1}M_\odot$ (dotted lines); $10^{13}h^{-1}M_\odot \leq M_S < 10^{14}h^{-1}M_\odot$ (dashed lines); and $M_S < 10^{13}h^{-1}M_\odot$ (dash-dotted lines). As one can see, the lensing signals in brighter bins are dominated by more massive haloes. Very massive haloes with $M_S \geq 10^{14}h^{-1}M_\odot$ are not the dominant contributor, even for the brightest luminosity bin considered here, because the total number of galaxies hosted by such haloes are relatively small. For the low-luminosity bins, relatively massive haloes dominate the ESD at large R , because a significant fraction of the low-luminosity satellites are hosted by massive haloes (see Figs. 2 and 3).

4.3 Dependence on Galaxy Type

In Fig. 6 we present the results separately for early-type and late-type galaxies. For a given luminosity bin, the predicted ESD has a higher amplitude for early-type galaxies, clearly due to the fact that early-type galaxies are more likely to reside in massive haloes (see e.g. van den Bosch, Yang & Mo 2003). For the faint samples, L1 and L2, the behavior of the predicted ESD for early-type galaxies resembles that of satellite galaxies in these luminosity bins, while the predicted ESD for the late-type galaxies looks like of the central galaxies in the corresponding luminosity bins. This, again, reflects the fact that faint early-type galaxies are mostly satellites in massive haloes, while the faint late-type population is dominated by the central galaxies in low-mass haloes.

The dashed lines in Fig. 6 show the results obtained using M_L as halo mass, rather than M_S (see § 3.2). For early-type galaxies, the results based on this halo mass estimate are very similar to those based on M_S . However, for the late-type samples, the ESDs obtained using M_L are significantly higher than those obtained using M_S , especially for the brighter samples. This is mainly due to the fact that late-type galaxies contain significant amounts of young stars, so that their stellar mass-to-light ratios are relatively low. Consequently, they are assigned a larger halo mass based on their luminosity than based on their stellar mass.

The model predictions are compared with the observational results of Mandelbaum et al. (2006). Here again, the model prediction based on M_S matches the observational data for the four bright samples. For the three faint bins, the model predictions are again lower than the observational results. As shown in Fig. 6, it seems that our model prediction agrees better with the observation for the late type galaxies.

For example, for L3 our model prediction matches the observation reasonably well for the late-type subsample (with the reduced χ^2 equal to 1.6), while the discrepancy is quite large for the early-type subsample (with reduced χ^2 equal to 5.3). Since faint, early-type galaxies are preferentially satellite galaxies in relatively massive halos while faint, late-type galaxies are mostly central galaxies in relatively low mass halos, the above results seem to indicate that the discrepancy is due to the underestimate of the 1-halo satellite term in the model. Unfortunately, there is no simple modification of the model that can fix the discrepancy. Since the spatial distribution of galaxies is fixed by the observation, the only change that can be made is in halo properties. As we will see in the following subsection, increasing the halo concentration even by a factor of two can only increase the predicted ESD by about 20% for the L3 sample, insufficient to explain the discrepancy. An increase in the halo masses assigned to galaxy groups can reduce the discrepancy for faint galaxies, but it would also significantly over-predict the ESD for bright galaxies. The other possibility is that the halo masses of isolated, faint early-type galaxies are significantly underestimated. For example, isolated early-type galaxies may reside in much more massive halos than that given by their stellar masses. In order to explain the discrepancy, the halo masses for these galaxies need to be larger by a factor of at least 3. This will not affect significantly the prediction for bright galaxies, but can boost the prediction for L3 by 50% at $R \sim 0.2h^{-1}\text{Mpc}$. Unfortunately, it is still unclear if the required halo mass increase is feasible in current models of galaxy formation.

4.4 Dependence on other Model Parameters

The ESD signal predicted by the model outlined in § 4.2 is based on several assumptions. Beside the underlying cosmology and the halo mass assignment which are the most crucial model ingredients (see § 4.5 and § 4.6), the model requires a concentration-halo mass relation and it assumes that central galaxies reside at rest at the centre of a *spherical* dark matter halo. In this subsection, we test how our results are affected by these assumptions.

The concentration parameter is a measure of the amount of dark matter in the central regions of the haloes. Accordingly, different models for the concentration-halo mass relations are expected to result in different predictions for the ESD signal (at least on small scales). The fiducial model described in § 4.2 uses the model of Macciò et al. (2007). However, other models are also available in the literature (e.g. Bullock et al. 2001; Eke, Navarro & Steinmetz 2001), which predict concentration-mass relations that are slightly different (see C08 for an assessment of the impact on galaxy-galaxy lensing). Furthermore, the presence of a (central) galaxy in a dark matter halo may have an impact on its concentration via, for example, adiabatic contraction (e.g. Blumenthal et al. 1986), which is not accounted for in the concentration-mass relations obtained from pure N -body simulations. Finally, attempts to measure halo concentrations observationally have thus far given conflicting results (e.g. van den Bosch & Swaters 2001; Comerford & Natarajan 2007, and references therein). To examine how the lensing predictions depend on changes in halo concentration we consider two models: model CH, in which the con-

centrations are 2 times as high as in our fiducial model, and model CL, in which the concentrations are 2 times smaller. The left column of Fig. 7 shows the predictions of models CH (dashed lines) and CL (dotted lines) compared to our fiducial model (solid lines). Results are only shown for four luminosity bins, as indicated. Note that the model with higher (lower) halo concentrations predicts ESDs that are higher (lower). The effect is stronger on scales where the 1-halo central term dominates (see Fig 4). Accordingly, in the case of the brightest sample (L6f), models CL and CH differ from the fiducial model on scales up to $R \simeq 1 h^{-1}\text{Mpc}$, while in sample L4 the differences are only appreciable out to $R \simeq 0.5 h^{-1}\text{Mpc}$. We conclude that the predicted ESD depends quite strongly on the assumed halo concentrations, indicating that galaxy-galaxy lensing has the potential to constrain the density profiles of dark matter haloes (see Mandelbaum et al. 2008). In this paper, we have assumed that the concentration of a halo depends only on its mass, we have ignored the possible halo age-dependence of the concentration-mass relation (e.g. Wechsler et al. 2002; Zhao et al. 2003; Lu et al. 2006). If for a given mass older halos have higher concentration, and if the formation of a galaxy in a halo depends strongly on the formation history of the halo, then the age-dependence of the halo concentration must be taken into account. Unfortunately, it is unclear how to connect the halo age (hence halo concentration) with the properties of galaxies. For a given halo mass, the dispersion in the concentration is about 0.12 dex (e.g. Jing 2000), which corresponds to a change of about 20% in the predicted ESD on $R \sim 0.1 h^{-1}\text{Mpc}$.

In our fiducial model, central galaxies are assumed to reside at the center of their dark matter haloes. However, as shown in van den Bosch et al. (2005), in haloes with masses $M_h > 10^{13} h^{-1} M_\odot$ there is evidence to suggest that central galaxies are offset from their halo centers by ~ 3 percent of the virial radius. A similar result was obtained by Berlind et al. (2003) using SPH simulations of galaxy formation. To examine how such an offset impacts on the ESDs, we consider two additional models. Following van den Bosch et al. (2005) and Yang et al. (2006), we assume that central galaxies in haloes with $M_S > 10^{13} h^{-1} M_\odot$ are offset from their halo centers by an amount that is drawn from a Gaussian distribution with zero mean. We use two different values for the dispersion of the distribution: 3% of the virial radius (model ‘Dev1’) and 6% of the virial radius (model ‘Dev2’). The corresponding lensing predictions are shown in the middle column of Fig. 7 as the dotted (Dev1) and dashed (Dev2) lines. Note that the offsets only affect the lensing signal for the brightest sample (L6f), where a larger offset results in a stronger suppression of the ESD on small scales ($R < 0.1 h^{-1}\text{Mpc}$). For fainter samples, no (significant) differences with respect to the fiducial model are apparent, which owes to the fact that fainter centrals typically reside in haloes with $M_h < 10^{13} h^{-1} M_\odot$ which do not have an offset (at least in our models).

As a final test, we examine the impact of halo shapes on the galaxy-galaxy lensing signal. In our fiducial model, dark matter haloes are assumed to be spherically symmetric. However, N -body simulations show that, in general, they are triaxial rather than spherical. Jing & Suto (1998) proposed a fitting formula for triaxial dark matter haloes, which has been applied to both strong and weak lensing analyses (e.g.

Oguri, Lee & Suto 2003; Oguri & Keeton 2004; Tang & Fan 2005). In order to examine the impact of our assumption of halo sphericity, we consider an alternative model (model ‘TRI’), in which we assume that the dark matter density distribution is given by $\rho_{\text{TRI}}(R)$, where R specifies an ellipsoidal surface:

$$R^2 = \left(\frac{x^2}{a^2} + \frac{y^2}{b^2} + \frac{z^2}{c^2} \right) c^2. \quad (10)$$

Here $a \leq b \leq c$ are the three principal semi-axes of the ellipsoid. We set $\rho_{\text{TRI}}(R) = \rho(R')$, where $\rho(R')$ is the NFW profile, so that the total mass within a sphere of radius R' in $\rho(R')$ is equal to the mass within the elliptical shell at R . For the axis ratios we adopt the distribution function given by Jing & Suto (2002):

$$p(a/c) = \frac{1}{\sqrt{2\pi} \times 0.113} \left(\frac{M_{\text{vir}}}{M_{NL}} \right)^{0.07[\Omega(z)]^{0.7}} \times \exp \left\{ - \frac{\left[(a/c)(M_{\text{vir}}/M_{NL})^{0.07[\Omega(z)]^{0.7}} - 0.54 \right]^2}{2(0.113)^2} \right\} \quad (11)$$

and

$$p(a/b|a/c) = \frac{3}{2(1 - \max(a/c, 0.5))} \times \left[1 - \left(\frac{2a/b - 1 - \max(a/c, 0.5)}{1 - \max(a/b, 0.5)} \right)^2 \right], \quad (12)$$

where M_{NL} is the characteristic mass scale, on which the rms of the top-hat smoothed over-density is equal to 1.68. In practice, we proceed as follows: For each dark matter halo we first draw the axis ratio a/c and a/b using Eqs. (11) and (12), respectively. Next we draw a random 3D orientation of the principal axes, and project the dark matter particles along the (fiducial) line-of-sight. Next, for each halo, we determine the major axis of the projected distribution which we align with the major axis of the central galaxy. This assumption is motivated by observational claims that the major axis of a central galaxy tends to be aligned with that of its host halo (e.g. Yang et al. 2006; Faltenbacher et al. 2008; Wang et al. 2008). As shown in the right-hand panels of Fig. 7, changing from spherical haloes (solid lines) to triaxial haloes (dotted lines) has almost no impact on the predicted ESDs. This should not come as an entire surprise, since the ESDs are azimuthally averaged over many haloes, which have random orientations on the sky. Note that here we assume that the halo is perfectly aligned with the central galaxy. However, the observational results mentioned above actually suggest a misalignment. We have tried a model in which the orientation of the host halo is uncorrelated with that of the central galaxy. The change in the results is very small compared with the model assuming perfect alignment.

4.5 Dependence on Cosmology

Another very important assumption in our model prediction is the cosmological model in the calculations of the halo mass function and the geometrical properties of spacetime. The redshifts of galaxies considered here are restricted to

$z \leq 0.2$, and the impact of changing cosmological parameters on the spacetime geometry is quite small in our analysis. On the other hand, changing cosmological parameters can change the halo masses assigned to individual groups, which may have significant impact on the expected lensing signal. In our fiducial model, we adopt the cosmology parameters obtained from the WMAP 3-year data, with $\Omega_m = 0.238$, $\Omega_\Lambda = 0.762$, $n = 0.951$, and $\sigma_8 = 0.75$ (Spergel et al. 2007). As comparison, we will show some results obtained assuming another set of cosmological parameters with $\Omega_m = 0.3$, $\Omega_\Lambda = 0.7$, $n = 1.0$, and $\sigma_8 = 0.9$, which is strongly supported by the first year data release of the WMAP mission (see Spergel et al. 2003) and has been considered in many previous studies. In what follows we will refer to this second set of parameters as the WMAP1 cosmology. Note that the cosmological parameters given by the recent WMAP 5-year data (Komatsu et al. 2008) are in between those of WMAP1 and WMAP3.

Fig. 8 compares the ESD predicted by the fiducial model using the WMAP3 cosmology (solid lines) and that predicted by the WMAP1 cosmology (dotted lines). As one can see, the ESD predicted by WMAP1 is significantly higher than that predicted by WMAP3, especially for bright galaxies. Most of this increase is due to changes in the halo mass function, which causes (massive) groups to be assigned a larger halo mass. The changes in the halo concentrations and the spacetime geometry play only a minor role. A comparison with the SDSS data clearly favors the WMAP3 cosmology over the WMAP1 cosmology, especially for the brighter luminosity bins. The reduced χ^2 for the WMAP1 cosmology is 21.3, much larger than 3.2 for the WMAP3 cosmology. This result is in good agreement with that obtained in C08 using the CLF model.

Thus, we conclude that the galaxy-galaxy lensing data either prefer the WMAP3 cosmology, which has a relatively low σ_8 , or our halo mass assignment is in serious error. In the following subsection we show that the uncertainties in our halo mass assignments are unlikely to change our results significantly. We therefore conclude that the galaxy-galaxy lensing data prefer a Λ CDM model with a relatively low σ_8 . If we use WMAP5 parameters, the model prediction is in between WMAP1 and WMAP3, which is still too high to match the observed ESD of bright galaxies.

4.6 Uncertainties in Halo-Mass Assignment

In our model, the masses of groups are assigned according to the stellar-mass ranking and the halo mass function predicted by the adopted cosmology. The underlying assumption is that the mass function of the host haloes of groups is the same as that predicted by the cosmological model. However, even if the cosmological model adopted is a good approximation to the real universe, the observed halo density may be different from the model prediction because of cosmic variance introduced by the finite observational volume. The effect of such variance is expected to be most important for massive haloes, because the number density of such systems is small. If, for example, the number density of massive haloes in the observational sample is, due to cosmic variance, smaller than the model prediction, the mass assignment with the use of the theoretical halo mass function would assign a higher halo mass to groups. Conse-

quently, the ESD of bright galaxies, which are biased toward massive haloes, would be overestimated. Here we test the importance of such effects by considering the uncertainties due to Poisson fluctuations. We use the halo mass function predicted with the WMAP3 cosmology to generate a set of random halo samples, each of which contains the same number of groups as the observational sample. The halo masses in each of these samples is then ranked in descending order and the halo mass of a given rank is then assigned to the group with the same rank in stellar mass. We find that the scatter in the ESD obtained in this way is negligibly small, even for the brightest sample. The reason is that, even for the brightest sample, the ESD is dominated by haloes with intermediate masses, $10^{13} h^{-1} M_\odot < M_S < 10^{14} h^{-1} M_\odot$ (see Fig. 5), and the total number of such groups is quite large.

Another uncertainty in the mass assignment may arise from fiber collisions. In the SDSS survey, no two fibers on the same SDSS plate can be closer than 55 arcsec. Although this fiber collision constraint is partially alleviated by the fact that neighboring plates have overlap regions, ~ 7 percent of all galaxies eligible for spectroscopy do not have a measured redshift. Our analysis here is based on the group catalog constructed from galaxy Sample II (see Y07), in which many of the galaxies missed due to fiber collisions are not included. Consequently, the total stellar mass (or the total luminosity) of some of the groups may be underestimated, thus introducing a bias in the ranking. This bias is expected to be stronger in richer systems because they have higher projected galaxy number density and are more likely to suffer from fiber collisions. However, this effect is not likely to have a big impact on our results, because it only changes the relative ranking of the groups that have similar stellar mass (luminosity) and because the galaxy-galaxy lensing signals are averaged in relatively broad bins of galaxy luminosity.

In order to quantify this effect we carry out a similar analysis using the group catalog constructed from Sample III, where a galaxy affected by fiber collisions is assigned the redshift of its nearest neighbor (see Y07 for details). In this case, the situation is the opposite to that in Sample II, because here some galaxies may be wrongly assigned to groups in the foreground or the background due to the wrong redshifts assigned to some of the fiber-collision galaxies. The stellar mass and the luminosity of some of the groups will therefore be overestimated. In our test, we use Sample III to construct the group and to set mass to groups according to their ranking in Sample III, but we calculate the ESD only around galaxies that are in Sample II. The results obtained in this way are very similar to those based on Sample II alone, suggesting that the effect of missing fiber-collision galaxies in the mass assignment is not important. However, if the fiber-collision galaxies are themselves included in the calculation of the ESD, i.e. if we use galaxies in Sample III to calculate the ESD, the amplitude of the ESD is significantly larger than that obtained from the galaxies in Sample II. The reason for this is that the galaxies affected by fiber collisions are preferentially located in high density regions, so that they are more likely associated with a massive halo. The observational results of Mandelbaum et al. (2006) are based on galaxies that have spectroscopic redshifts, and so a fair comparison between the observational results and our model predictions can only be made with the use of galaxies in Sample II. Our test above therefore demonstrates that

our conclusions about the comparison between the observational data and the model predictions are robust against the uncertainties due to fiber collisions.

The scatter in the relation between halo mass and stellar mass (or luminosity) may also produce some uncertainties in our model prediction. As shown in Mandelbaum & Seljak (2007), the scatter is in partial degeneracy with cosmology model. In our investigation, we have fixed cosmological parameters and allowed no dispersion in the halo mass-total stellar mass relation. If, for example, we assume a log normal distribution with a dispersion of 0.3 index in halo mass for a given stellar mass, the predicted ESD would be a few percent larger than that predicted by the fiducial model.

5 SUMMARY

In this paper we model the galaxy-galaxy lensing signal expected for SDSS galaxies, using the galaxy groups selected from the SDSS to represent the dark matter haloes within which the galaxies reside. We use the properties of the dark halo population, such as mass function, density profiles and shapes, expected from the current Λ CDM cosmogony to model the dark matter distribution in each of the groups identified in the SDSS volume. The use of the real galaxy groups allows us to predict the galaxy-galaxy lensing signals separately for galaxies of different luminosity, morphological types, and in different environments (e.g. central versus satellite galaxies). We check the robustness of our model predictions by changing the assumptions about the dark matter distribution in individual groups (such as the shape, density profile, and center offset of dark matter haloes), as well as the cosmological model used to predict the properties of the halo population. We compare our model predictions with the observational data of Mandelbaum et al. (2006) for similar samples of lens galaxies. Although there is some discrepancy for lens galaxies in the low-luminosity bins, the overall observational results can be well understood in the current Λ CDM cosmogony. In particular, the observed results can be well reproduced in a Λ CDM model with parameters based on the WMAP3 data, but a Λ CDM model with a significantly higher σ_8 , such as the one based on the WMAP1 data, significantly over-predicts the galaxy-galaxy lensing signal. Our results also suggest that, once a correct model of structure formation is adopted, the halo masses assigned to galaxy groups based on ranking their stellar masses with the halo mass function, are statistically reliable. The results obtained imply that galaxy-galaxy lensing is a powerful tool to constrain both the mass distribution associated with galaxies and cosmological models. In the future, when deep imaging surveys provide more sources with high image quality in the SDSS sky coverage, the galaxy-galaxy lensing signals produced by the SDSS galaxies can be estimated to much higher accuracy. The same analysis as presented here is expected to provide stringent constraints on the properties of the dark matter haloes associated with galaxies and galaxy systems, as well as on cosmological parameters.

ACKNOWLEDGMENTS

We thank Rachel Mandelbaum for providing the SDSS lensing data in electronic format. Part of the computation was carried out on the SGI Altix 330 system at the Department of Astronomy, Peking University. Li Ran is supported by the National Scholarship from China Scholarship Council. XY is supported by the *One Hundred Talents* project of the Chinese Academy of Sciences and grants from NSFC (Nos. 10533030, 10673023). HJM would like to acknowledge the support of NSF AST-0607535, NASA AISR-126270 and NSF IIS-0611948. Zuhui Fan would like to acknowledge the supports from NSFC under grants. 10373001, 10533010, and 10773001, and 973 Program (No. 2007CB815401).

REFERENCES

- Adelman-McCarthy J. K., et al., 2006, ApJS, 162, 38
- Bell E. F., McIntosh D. H., Katz N., Weinberg M. D., 2003, ApJS, 149, 289
- Berlind, A. A., Weinberg D. H., 2002, ApJ, 575, 587
- Berlind A. A., et al., 2003, ApJ, 593, 1
- Blanton M. R., et al., 2003, AJ, 125, 2348
- Blanton M. R., et al., 2005, AJ, 129, 2562
- Blumenthal G. R., Faber S. M., Flores R., Primack J. R., 1986, ApJ, 301, 27
- Brainerd T. G., Blandford R. D., Smail I., 1996, ApJ, 466, 623
- Bullock J. S., Kolatt T. S., Sigad Y., Somerville R. S., Kravtsov A. V., Klypin A. A., Primack J. R., Dekel A., 2001 MNRAS, 321, 559
- Cacciato M., van den Bosch F. C., More S., Li R., Mo H. J., Yang X., 2008, submitted to MNRAS (C08)
- Cole S., Lacey C.G., Baugh C.M., Frenk C.S., 2000, MNRAS, 319, 168
- Colless M., et al., 2001, MNRAS, 328, 1039
- Comerford J. M., Natarajan P., 2007, MNRAS, 379, 190
- Cooray A., Sheth R., 2002, PhR, 372, 1
- Cooray A., 2006, MNRAS, 365, 842
- Croton D. J., et al., 2006, MNRAS, 367, 864
- de Vaucouleurs G., de Vaucouleurs A., Corwin H.G., Buta R.J., Paturel G., Fouque P., 1991, Third Reference Catalogue of Bright Galaxies, (Springer-Verlag Heidelberg)
- Eke V.R., Navarro J.F., Steinmetz M., 2001, ApJ, 554, 114
- Faltenbacher A., Li C., Mao S., van den Bosch F. C., Yang X., Jing Y. P., Pasquali A., Mo H. J., 2007, ApJ, 662, 71
- Giocoli C., Tormen G., van den Bosch F.C., 2008, MNRAS, 386, 2135
- Gao L., White S. D. M., Jenkins A., Stoeckl F., Springel V., 2004, MNRAS, 355, 819
- Hayashi E., Navarro J. F., Taylor J. E., Stadel J., Quinn T., 2003, ApJ, 584, 541
- Henry, J. P., 2000, ApJ, 534, 565
- Hoekstra H., Franx M., Kuijken K., Carlberg R. G., Yee H. K. C., 2003, MNRAS, 340, 609
- Hoekstra H., 2004, MNRAS 347, 1337
- Hudson M. J., Gwyn S. D. J., Dahle H., Kaiser N., 1998, ApJ, 503, 531
- Jing Y. P., Suto, Y., 1998, ApJ, 494L, 5
- Jing Y. P., 2000, ApJ, 535, 30
- Jing Y. P., Suto Y., 2002, ApJ, 574, 538

- Jing Y. P., Mo H. J., Börner G., 1998, *ApJ*, 494, 1
- Johnston D. E., et al., 2007, preprint (arXiv: astro-ph/0709.1159)
- Kang X., Jing Y. P., Mo H. J., Börner G., 2005, *ApJ*, 631, 21
- Kauffmann G., White S. D. M., Guiderdoni B., 1993, *MNRAS*, 264, 201
- Kauffmann G., White S. D. M., Heckman T. M., Menard B., Brinchmann J., Charlot S., Tremonti C., Brinkmann J. 2004, *MNRAS*, 353, 713
- Katz N., Weinberg D. H., Hernquist L., 1996, *ApJS*, 105, 19
- Komatsu E., Dunkley J., 2008, preprint (arXiv: astro-ph/0803.0547)
- Limousin M., Kneib J. P., Bardeau S., Natarajan P., Czoske O., Smail I., Ebeling H., Smith G.P., 2007, *A&A*, 461, 881
- Lu Y., Mo H. J., Katz N., Weinberg M. D., 2006, *MNRAS*, 368, 1931
- Macciò A. V., Dutton A. A., van den Bosch F. C., Moore B., Potter D., Stadel J., 2007, *MNRAS*, 378, 55.
- Mandelbaum R., et al., 2005, *MNRAS*, 361, 1287
- Mandelbaum R., Seljak U., Kauffmann G., Hirata C. M., Brinkmann J., 2006 *MNRAS*, 368, 715
- Mandelbaum R., Seljak, U., 2007, *JACP*, 06, 024
- Mandelbaum R., Seljak, U., Hirata C. M., 2008, preprint (arXiv: astro-ph/0805.2552)
- McKay T. A., Sheldon E. S., Racusin J., et al. 2001, preprint (arXiv: astro-ph/0108013)
- McKay T. A., et al., 2002, *ApJ*, 571, L85
- Nakamura T. T., Suto Y., 1997, *PThPh*, 97, 49
- Natarajan P., Kneib J.P., Smail I., 2002, *ApJ*, 580, L11
- Navarro J.F., Frenk C.S., White S.D.M., 1997, *ApJ*, 490, 493
- Oguri M., Lee J., Suto Y., 2003, *ApJ*, 599, 7
- Oguri M., Keeton C., 2004, *ApJ*, 610, 663
- Peacock J. A., Smith R. E., 2000, *MNRAS*, 318, 1144
- Pearce F. R., Thomas P. A., Couchman H. M. P., Edge A. C., 2000, *MNRAS*, 317, 1029
- Petrosian V., 1976, *ApJ*, 209, L1
- Saunders W., et al., 2000, *MNRAS*, 317, 55
- Scranton R., 2003, *MNRAS* 339, 410
- Schlegel D.J., Finkbeiner D.P., Davis M., 1998, *ApJ*, 500, 525
- Sheldon E. S., et al., 2004, *AJ*, 127, 2544
- Sheldon E. S., et al., 2007a, preprint (arXiv:astro-ph/0709.1153)
- Sheldon E. S., et al., 2007b, preprint (arXiv: astro-ph/0709.1162)
- Somerville R. S., Primack J. R., 1999, *MNRAS*, 310, 1087
- Spergel D. N., et al., 2003, *ApJS*, 148, 175
- Spergel D. N., et.al., 2007, *ApJS*, 170, 377
- Springel V., 2005, *MNRAS*, 364, 1105
- Springel V., et al., 2005, *Nature*, 435, 629
- Strauss M.A., et al., 2002, *AJ*, 124, 1810
- Tang J. Y., Fan Z. H., 2005, *ApJ*, 635, 60
- Tinker J.L., Weinberg D.H., Zheng Z., Zehavi I., 2005, *ApJ*, 631, 41
- Tyson J. A., Valdes F., Jarvis J. F., Mills A. P. Jr., 1984, *ApJ*, 281L, 59
- Vale A., Ostriker J. P., 2006, *MNRAS*, 371, 1173
- van den Bosch F. C., Swaters R. A., 2001, *MNRAS*, 325, 1017
- van den Bosch F. C., 2002, *MNRAS*, 332, 456
- van den Bosch F. C., Yang X., Mo H. J., 2003, *MNRAS*, 340, 771
- van den Bosch F. C., Norberg P., Mo H. J., Yang X., 2004, *MNRAS*, 352, 1302
- van den Bosch F. C., Weinmann S. M., Yang X., Mo H. J., Li C., Jing Y.P., 2005, *MNRAS*, 361, 1203
- van den Bosch F. C., Tormen G., Giocoli C., 2005, *MNRAS*, 359, 1029
- van den Bosch F. C., et al., 2007, *MNRAS*, 376, 841
- Wang Y., Yang X., Mo H. J., Li C., van den Bosch F. C., Fan Z. H., Chen X., 2008, *MNRAS*, 385, 1511
- Warren M. S., Abazajian K., Holz D. E., Teodoro L., 2006, *ApJ*, 646, 881
- Wechsler R. H., Bullock J. S., Primack J. R., Kravtsov A. V., Dekel A., 2002, *ApJ*, 568, 52
- Weinberg D. H., Colombi S., Davè R., Katz N., 2008, *ApJ*, 678, 6
- White S. D. M., Frenk C., 1991, *ApJ*, 379, 52
- Yan R., Madgwick D. S., White M., *ApJ*, 2003, 598, 848
- Yang X., Mo H. J., van den Bosch F. C., 2003, *MNRAS*, 339, 1057
- Yang X., Mo H. J., van den Bosch F. C., Jing Y. P., 2005, *MNRAS*, 356, 1293
- Yang X., Mo H. J., van den Bosch F. C., Jing Y. P., Weinmann S. M., Meneghetti M., 2006, *MNRAS*, 373, 1159
- Yang X., Mo H. J., van den Bosch F. C., Pasquali A., Li C., Barden M., 2007, *ApJ*, 671, 153 (Y07)
- Yang X., Mo H. J., van den Bosch F. C., 2008, preprint, (arXiv: astro-ph/0808.0539)
- Zhao D. H., Jing Y. P., Mo H. J., Börner G., 2003, *ApJ*, 597, 9
- Zheng Z., et al., 2005, *ApJ*, 633, 791
- Zheng Z., Weinberg D. H., 2007, *ApJ*, 659, 1